A Novel Method for the Low-detectable Dihedral Corner Utilizing Phase Gradient Metasurface based on Phase Cancellation Mechanism

Qingting He[1], Jianliang Xie[1], Qian Liu[1], Xin Yao[1], Zhi Wang[2], Haiyan Chen[1*], Fengxia Li[3], and Longjiang Deng[1]

[1]National Engineering Research Center of Electromagnetic Radiation Control Materials
Key Laboratory of Multi-Spectral Absorbing Materials and Structures of Ministry of Education
State Key Laboratory of Electronic Thin Films and Integrated Devices
University of Electronic Science and Technology of China, Chengdu, 611731, People's Republic of China
hqt@std.uestc.edu.cn, jlxie@uestc.edu.cn, lq96@std.uestc.edu.cn, 2835025811@foxmail.com,
*chenhy@uestc.edu.cn, dfliang@uestc.edu.cn, denglj@uestc.edu.cn

[2]Glasgow College, University of Electronic Science and Technology of China
Chengdu, 610054, People's Republic of China
2019190503033@std.uestc.edu.cn

[3]School of Physics and Optoelectronic Engineering, Xidian University
Xi'an, 710071, People's Republic of China
lifengxia@xidian.edu.cn

***Abstract* –** In this paper, a phase gradient metasurface (PGM) is proposed to reduce the radar cross-section (RCS) of the dihedral corner based on phase cancellation mechanism. The phase cancellation mechanism is used to derive the formula of the low-detectable dihedral corner for the first time, which is directly used to deal with the wave path difference problem that introduced by the dihedral corner. According to the formula, six sub-cells are designed with a 60° phase difference, which is arranged by sub-array along the y-axis. The reflection coefficients of the selected sub-cells are all above 0.8. The RCS reduction of the dihedral corner achieves over 10 dB from 4.9 GHz to 5.14 GHz under an incident angle of 45°. In particular, the RCS reduction of the low-detectable dihedral corner is 13.97 dB at 5 GHz. Meanwhile, the proposed dihedral corner with PGM also has an excellent performance of angle insensitivity ranging from 0° to 75°. To further verify our design, the dihedral corner with PGM is manufactured by a low-cost printing circuit board technique. The measured results agreed well with the simulations, and both of them show an excellent performance of RCS reduction in the operating frequency band, regardless of any angle within 75°. Overall, the dihedral corner with PGM that we proposed has the advantages of being low-detectable, low-profile, low-cost, lightweight, and it is easy to design and manufacture. It has wide application prospects in the future.

***Index Terms* –** low-detectable dihedral corner, low-profile metasurface, phase cancellation, phase gradient metasurfaces, radar cross-section, wave path difference.

I. INTRODUCTION

The dihedral corner, which normally forms between the aircraft's tails, is a typical scattering structure of a radar target. Its feature recognition is of crucial significance for detecting complicated targets, and it also serves as the basis for researching the scattering properties of gradual scatters. In the design of low-detectable targets, the dihedral corner is a significant scattering source, and it is critical to regulate its scattering characteristics. At present, the control methods for dihedral corner scattering characteristics mainly include the loading of lossy materials [1–2], optimization of the included angle of the dihedral corner [3–4], passive loading [5–6], etc.

Metasurface [7–9] is a sub-wavelength unit with special manipulability for amplitude, phase, and polarization of electromagnetic (EM) waves, which has been applied in many fields, such as metalenses [10–11], perfect absorbers [12–13], holograms [14–15], polarization controllers [16–17], anomalous reflection [18–19], and radar cross-section (RCS) reduction [20–21]. As an important type of metasurface, phase gradient metasurface (PGM) consists of a series of phase discontinue cells, which were first mentioned

Submitted On: October 9, 2022
Accepted On: May 10, 2023

https://doi.org/10.13052/2023.ACES.J.380406

by Yu [22]. In [22], it generates an optical vertices beam by constructing eight different reflection angles. Thenceforth, PGM has gained extensive attention [23–25]. By regulating the phase gradient of PGM, the wavefront of the electromagnetic wave can be changed as needed, so that PGM provides another method for the scattering control of the dihedral corner. However, the research on RCS reduction of PGM is mainly focused on the flat [23–25]. As far as we know, PGM is hardly ever used for the RCS reduction design of the dihedral corner [9]. An approach to achieve RCS reduction of the dihedral corner where the RCS is determined by multiple-bounce mechanisms is proposed [9]. The suggested method additionally makes use of array theory to specify precise guidelines to avoid grating lobes [9]. Nevertheless, they ignored the issue of the wave path difference that the dihedral corner itself introduced. According to the related researches, the wave path difference is particularly important to solve the RCS reduction of the dihedral corner, and it is necessary to carry out this research in-depth.

In this paper, the method of phase cancellation, by combining the wave path difference between two planes of the dihedral corner with the phase gradient of the PGM was presented to control the RCS of the dihedral corner. The formula of the low-detectable dihedral corner, which directly addresses the wave path difference issue that the dihedral corner itself introduces, is derived based on phase cancellation mechanism for the first time. The working principle is given in detail. The RCS reduction of the dihedral corner with PGM achieves over 10 dB between 4.9 GHz and 5.14 GHz at a 45° incidence angle. In particular, the RCS reduction of the low-detectable dihedral corner is 13.97 dB at 5 GHz. Furthermore, the suggested dihedral corner with PGM shows outstanding property in terms of angle insensitivity between 0° and 75°. Above all, simulation and measurement demonstrate that our method can reduce the dihedral corner's RCS. The dihedral corner with PGM has potential applications in reducing the RCS of the dihedral corner.

II. DESIGN AND SIMULATION

The dihedral corner usually consists of two perfect electric conductors (PECs) in xoy and yoz planes, as shown in Fig. 1. When the plane wave is incident on PEC along yoz at 45°, it will be reflected onto the xoy plane according to generalized Snell's law. Due to differing propagation pathways, the phase difference will appear, resulting in a strong scattering far-field, this will increase the possibility of detecting. To solve this problem, PGM is intended to replace PEC in the xoy plane to compensate for wave path difference, providing a sequence of continuous phase abrupt of variable

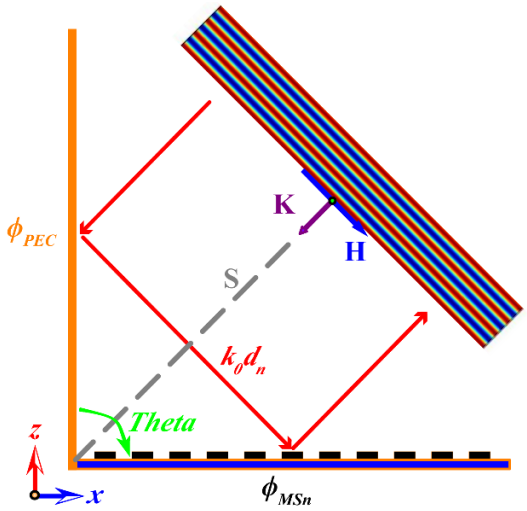

Fig. 1. Schematic of the working principle of the low-detectable dihedral corner.

size. According to the passive cancellation principle, scattering performance will rapidly decrease with a reasonable phase arrangement. The detailed design flows are as follow.

Assuming the periodicity of the sub-unit cell of PGM is p, the distance between the center point of the nth unit cell (xoy plane) and its mirror point (yoz plane) about the symmetry plane S is

$$d_n = \frac{\sqrt{2}(2n-1)}{2}p, \tag{1}$$

where n is the position of the nth unit cell.

The plane wave incidences dihedral corner at 45°. Using the principle of phase cancellation, we can derive Equation 2,

$$\phi_{MSn} + k_0 d_n - \phi_{PEC} = \pi + 2M\pi, \tag{2}$$

where ϕ_{MSn} and ϕ_{PEC} are the phases of the metasurface and PEC of the nth cell, respectively, $k_0 = 2\pi/\lambda_0$ is the propagation constant, λ_0 is the wavelength in free space, and M is an integer.

The reflection phase of PEC is $-\pi$, the corresponding phase of the unit cell of the PGM that needs to be designed is deduced as

$$\phi_{MSn} = -\sqrt{2}(2n-1)\pi\frac{p}{\lambda_0} + 2(m+1)\pi. \tag{3}$$

The phase shift between adjacent cells of PGM can be derived

$$d\phi = \phi_{MS(n-1)} - \phi_{MSn} = 2\sqrt{2}\pi\frac{p}{\lambda_0}. \tag{4}$$

It can be seen from Equation (3) that we can reduce the RCS of the dihedral corner by adjusting the phase of PGM, and the phase difference between adjacent sub-units can be determined by Equation (4).

A reflective low-profile metasurface is chosen here, which is a typical sandwich structure. The proposed

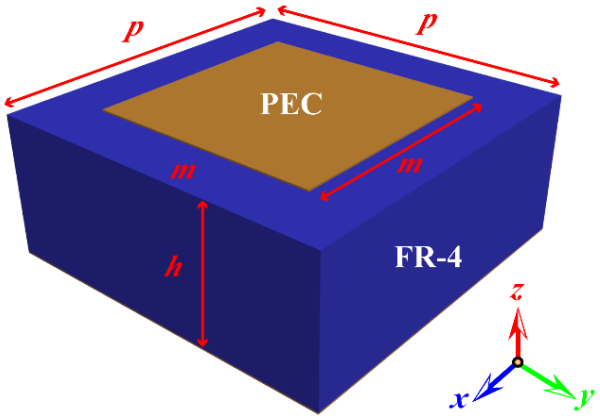

Fig. 2. Schematic illustration of the unit cell structure of metasurfaces with variable *m*.

unit cell is the type of sub-wavelength structure, and its parameters are shown in Fig. 2. The top layer is a simple copper square patch with conductivity of 5.8×10^7 S/m with length of *m*. The FR-4 substrate backed by PEC plane has thickness of $h = 3$ mm ($0.05\lambda_0$) with dielectric constant of 4.3 and loss tangent of 0.025, and the period of the cell is $p = 7.07$ mm. The phase of the metasurfaces can be adjusted by changing the parameter *m*.

To get the desired phase gradient, parameter *m* is swept by the numerical calculation software CST Studio Suite. In the simulation setup, the EM waves are incident at a 45° angle. The boundary condition is unit cell along the *x*- and *y*-axis, and open (add space) boundary along the *z*-direction. The reflection phase and the detailed geometrical parameters *m* of six sub-cells are listed at 5 GHz in Table 1. From Table 1, it can be seen that the phase difference between adjacent cells is almost 60°. In the local enlarged image of Fig. 3, the supercell of PGM is composed by these six sub-cells.

Table 1: The reflection phase and the geometrical parameters *m* of the six unit cells at 5 GHz

N	1	2	3	4	5	6
m (mm)	6.7	6.83	7.02	2.72	6.33	6.58
Phase (°)	329.89	269.46	209.90	150.23	89.53	29.95

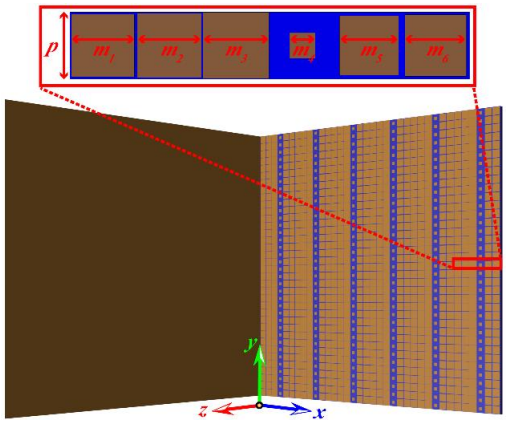

Fig. 3. Schematic diagram of the dihedral corner with metasurface. The local enlarged image corresponding to the red frame above the picture is the supercell of the designed metasurface.

All cells have a strong reflection due to the existence of PEC ground. As illustrated in Fig. 4 (a), the reflection amplitude of six sub-cells exceeds 0.8 in the simulation frequency band. Additionally, the reflection phase can cover 360° by changing the values of *m*, as shown in Fig. 4 (b).

The supercell is periodically arranged to form the PGM with the size of 254.52 mm × 254.52 mm, which is composed of 36 × 36 unit cells. In Fig. 3, we show the

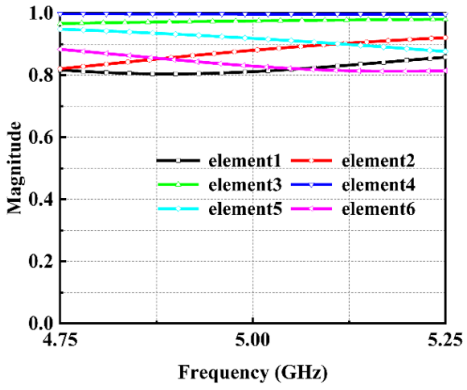

(a)

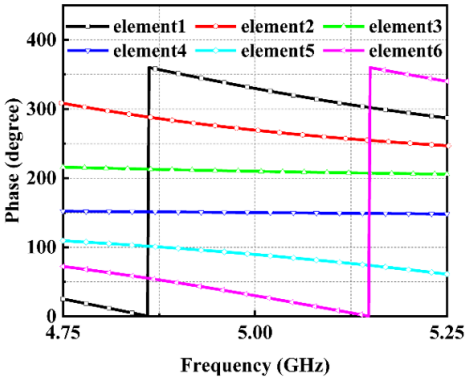

(b)

Fig. 4. Simulated reflection coefficients for the unit cells with the change of *m*, at 5 GHz, (a) amplitude and (b) phase.

dihedral corner with PGM, which is composed of PGM in the xoy plane, and the copper plate is designed with the same size in the yoz plane.

III. SIMULATION RESULTS AND DISCUSSION

To better validate the method mentioned above, the RCS of the dihedral corner with and without PGM are simulated. The dihedral corner without PGM serves as the comparison group, which only consists of metal plates. Figure 5 shows the RCS of the dihedral corner with and without PGM under transverse electric (TE) polarization wave impinging at 45°. As seen in Fig. 5, the RCS of the dihedral corner with a low-profile metasurface is significantly lower than the comparison group in the frequency range of 4.75 GHz to 5.25 GHz. The RCS reduction of the dihedral corner achieves over 10 dB from 4.9 GHz to 5.14 GHz. According to Fig. 5, the RCSs of the dihedral corner without and with PGM at 5 GHz are 13.1 dB and -0.87 dB, respectively. This means the RCS reduction of the low-detectable dihedral corner is 13.97 dB at 5GHz. The simulation results demonstrate that over 10 dB RCS reduction (RCSR) is realized at 5 GHz, which is virtually in line with the above estimate.

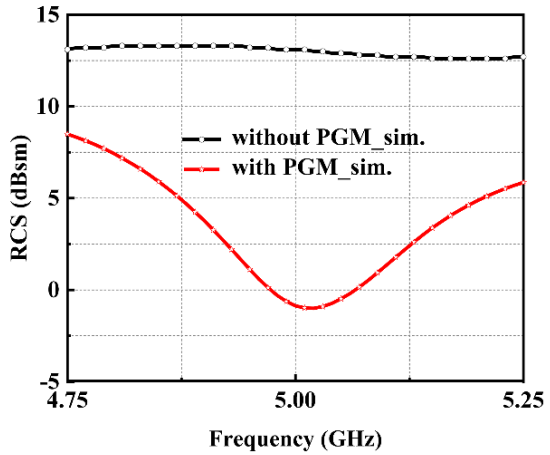

Fig. 5. Simulated RCS of the dihedral corner with and without PGM at 45° oblique incidence at different frequencies.

To further evaluate the RCSR performance, the monostatic RCS under oblique incidence is simulated at 5 GHz. As shown in Fig. 6, RCS is reduced with the variation of the incident angle range from 0° to 75°. As a result, the proposed dihedral corner with PGM has outstanding RCS reduced performance across a specific angle range.

To better understand the mechanism of RCS reduction, the 3D bistatic scattering patterns of the

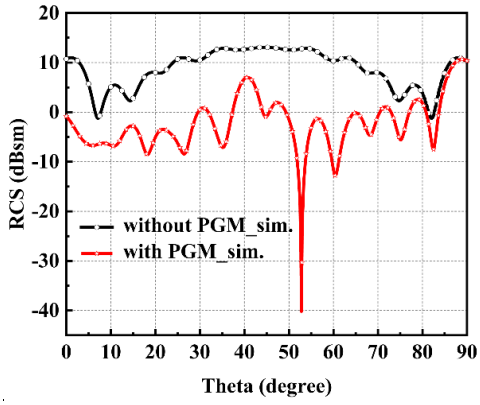

Fig. 6. Simulated RCS of the dihedral corner with and without PGMs at 5 GHz at different azimuth angle.

dihedral corner with and without PGM are illustrated when the incident angle is 45° and the operation frequency is at 5 GHz, as shown in Fig. 7. The RCSs of the dihedral corner without and with PGM are 13.1 dB and -0.87 dB, respectively. The reflected energy of the dihedral corner without PGM is centered on the main lobe, as shown in Fig. 7 (a). On the contrary, the main lobe is split, and the magnitude has a significant reduction when PGM is loaded, as seen in Fig. 7 (b). According to the energy conservation principle, the main lobe of the dihedral corner with PGM is effectively suppressed. Therefore, the dihedral corner with the purposed PGM has the property of RCS reduction.

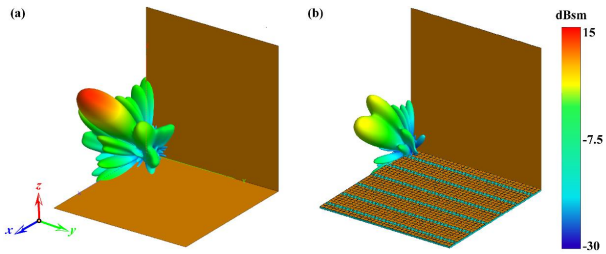

Fig. 7. 3D bistatic scattering pattern of the dihedral corner under oblique incidence angle at 45° at 5 GHz, (a) without metasurface and (b) with metasurface.

IV. MEASUREMENT RESULTS

To further verify our design, a sample with a size of 254.52 mm × 254.52 mm is manufactured by low-cost printing circuit board (PCB) technology. Figure 8 exhibits the photograph of the sample with a zoomed view of the 1 × 6 array of PGM's supercell. The RCS of the sample is measured in the microwave anechoic chamber. The measured results are compared at various frequencies when the plane wave is incident at 45°.

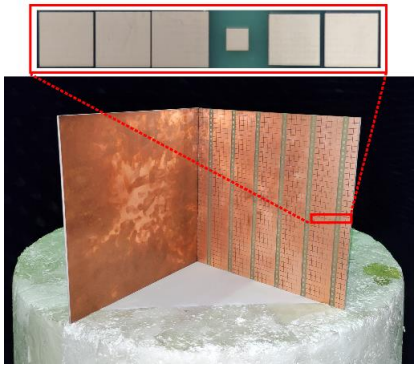

Fig. 8. The photograph of the manufactured sample. The local enlarged image corresponding to the red frame above the picture is the supercell of the designed metasurface.

To verify the accuracy of the measurement, we replot the simulation results in Fig. 9. The experimental results are in good agreement with the simulation results. The experimental results demonstrate that the RCS of the dihedral corner with PGM is obviously lower than the dihedral corner without PGM in the frequency range of 4.75 GHz to 5.25 GHz. The RCS reduction of the dihedral corner achieves over 10 dB from 4.95 GHz to 5.11 GHz. In Fig. 5, the RCSs of the dihedral corner without and with PGM are 12.03 dB and -1.08 dB at 5 GHz, respectively. Namely, the RCS reduction of the low-detectable dihedral corner is 13.05 dB at 5GHz. From Fig. 9, the results of simulations and measurements show that over 10 dB RCSR is achieved at 5 GHz, which is essentially in line with the aforementioned design.

Meanwhile, to assess the RCSR's performance, we measured the RCS of the dihedral corner with and without PGM at 5 GHz at different azimuth angles.

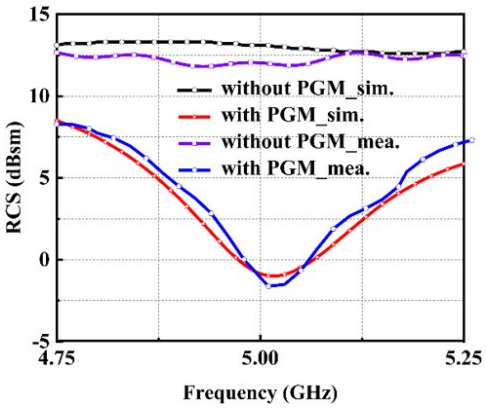

Fig. 9. Simulated and measured RCS of the dihedral corner with and without PGM at 45° oblique incidence at different frequencies.

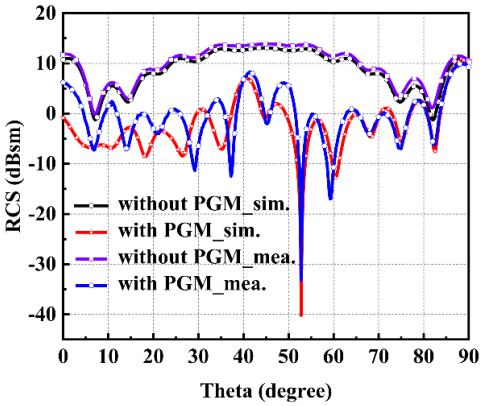

Fig. 10. Simulated and measured RCS of the dihedral corner with and without PGM at 5GHz at different azimuth angles.

Similar to Fig. 9, we display the simulation results in Fig. 10. The sample shows excellent angle insensitivity performance in the range of 0° to 75°, as illustrated in Fig. 10. Both of them agree well with simulation results, with slight deviations due to manufacturing and measurement errors. Above all, the measurements corroborate our method and demonstrate that our design can reduce the RCS of the dihedral corner.

V. CONCLUSION

In this paper, a novel design method has been proposed to reduce the RCS of the dihedral corner according to the principle of phase cancellation combined with PGM. With the loading of a low-profile metasurface ($0.05\lambda_0$) on the dihedral corner, phase cancellation is performed directly on the wave path difference introduced by the dihedral structure itself, to achieve RCS reduction of the dihedral corner. The guidance formula of a low-detectable dihedral corner based on phase cancellation mechanism is derived for the first time, which directly solves the wave path difference issue due to the dihedral corner structure itself. According to the guiding formula, six different phase reflection sub-cells are designed with 60° phase differences. Low-detectable dihedral corners are demonstrated to be effective in reducing the backscattered power utilizing the simulation of RCS and 3D bistatic scattering patterns. Both simulation and experiment show an excellent RCS reduction over 10 dB at 5 GHz with a 45° incident angle. Moreover, the PGM is still effective when the incidence angle ranges from 0° to 75°. This study provides a novel and meaningful approach to design a low-RCS dihedral corner, which can be applied to complex electromagnetic regulation scenarios. The low-detectable dihedral corner also has the benefit of being lightweight because it only requires one-sided loading with the low-profile metasurface,

which was manufactured by a low-cost PCB technique. To verify the effectiveness of the method, we only show its application in the microwave band. Actually, the method can be used at any frequency. Furthermore, the method does not entail absorbing materials. So, it has the potential to be used in high-temperature settings.

ACKNOWLEDGMENT

This work was supported by the National Natural Science Foundation of China (No. 52021001 and 51972046)) and Strategic research and consulting project of Chinese Academy of Engineering (NO.2022-XY-127), and partly supported by Program for Changjiang Scholars and Innovative Research Team in University (PCSIRT).

REFERENCES

[1] T. Griesser, C. A. Balanis, and K. Liu, "RCS analysis and reduction for lossy dihedral corner reflectors," *Proc. IEEE.*, vol. 77, pp. 806-814, 1989.

[2] Y. Hingcheng and H. Peikang, "Po analysis for RCS of nonorthogonal dihedral corner reflectors coated by RAM," *J. Syst. Eng. Electron.*, vol. 12, pp. 1-6, 2001.

[3] E. Knott, "RCS reduction of dihedral corners," *IEEE Trans. Antennas Propag.*, vol. 25, pp. 406-409, 1977.

[4] D. K. Atwood and L. Thirion-Lefevre, "Polarimetric phase and implications for urban classification," *IEEE Trans. Geosci. Remote Sens.*, vol. 56, pp. 1278-1289, 2018.

[5] A. Y. Modi, C. A. Balanis, C. R. Birtche, and H. N. Shaman, "New class of RCS-reduction metasurfaces based on scattering cancellation using array theory," *IEEE Trans. Antennas Propag.*, vol. 67, pp. 298-308, 2019.

[6] A. Y. Modi, M. A. Alyahya, C. A. Balanis, and C. R. Birtcher, "Metasurface-based method for broadband RCS reduction of dihedral corner reflectors with multiple bounces," *IEEE Trans. Antennas Propag.*, vol. 68, pp. 1436-1447, 2020.

[7] G. Liu, J. Han, X. Gao, H. Liu, and L. Li, "A novel frequency reconfigurable polarization converter based on active metasurface," *Applied Computational Electromagnetics Society (ACES) Journal*, vol. 34, pp. 1058-1063, 2019.

[8] L. N. Nguyen, "A new metasurface structure for bandwidth improvement of antenna array," *Applied Computational Electromagnetics Society (ACES) Journal*, vol. 36, pp. 139-144, 2021.

[9] A. A. Abbas and B. S. Samet, "A compact high gain wideband metamaterial antenna for sub-6 GHz applications," *Applied Computational Electromagnetics Society (ACES) Journal*, vol. 37, pp. 886-89, 2022.

[10] Y. Meng, Y. Chen, L. Lu, Y. Ding, A. Cusano, J. A. Fan, Q. Hu, K. Wang, Z. Xie, Z. Liu, Y. Yang, Q. Liu, M. Gong, Q. Xiao, S. Sun, M. Zhang, X. Yuan, and X. Ni, "Optical meta-waveguides for integrated photonics and beyond," *Light Sci. Appl.*, vol. 10, pp. 235, 2021.

[11] Y. Wang, Q. Chen, W. Yang, Z. Ji, L. Jin, X. Ma, Q. Song, A. Boltasseva, J. Han, V. M. Shalaev, and S. Xiao, "High-efficiency broadband achromatic metalens for near-IR biological imaging window," *Nat. Commun.*, vol. 12, pp. 5560, 2021.

[12] Y. Yao, R. Shankar, M. A. Kats, Y. Song, J. Kong, M. Loncar, and F. Capasso, "Electrically tunable metasurface perfect absorbers for ultrathin mid-infrared optical modulators," *Nano Lett.*, vol. 14, pp. 6526-6532, 2014.

[13] A. Tittl, A.-K. U. Michel, M. Schäferling, X. Yin, B. Gholipour, L. Cui, M. Wuttig, T. Taubner, F. Neubrech, and H. Giessen, "A switchable mid-infrared plasmonic perfect absorber with multispectral thermal imaging capability," *Adv. Mater.*, vol. 27, pp. 4597-4603, 2015.

[14] X. Ni, A. V. Kildishev, and V. M. Shalaev, "Metasurface holograms for visible light," *Nat. Commun.*, vol. 4, Art. no. 2807, 2013.

[15] G. Zheng, H. Mühlenbernd, M. Kenney, G. Li, T. Zentgraf, and S. Zhang, "Metasurface holograms reaching 80% efficiency," *Nat. Nanotechnol.*, vol. 10, pp. 308-312, 2015.

[16] N. K. Grady, J. E. Heyes, D. R. Chowdhury, A. R. Dalvit, and A. Chen, "Terahertz metamaterials for linear polarization conversion and anomalous refraction," *Science*, vol. 340, pp. 1304-1307, 2013.

[17] B. Kamal, J. Chen, Y. Yingzeng, J. Ren, S. Ullah, and W. U. R. Khan, "High efficiency and ultra-wideband polarization converter based on an L-shaped metasurface," *Opt. Mater. Express.*, vol. 11, pp. 1343-1352, 2021.

[18] G. Dong, Z. Jiang, and Y. Li, "Large asymmetric anomalous reflection in bilayer gradient metasurfaces," *Opt. Express.*, vol. 29, pp. 16769-16780, 2021.

[19] M. B. Soley, K. N. Avanaki, and E. J. Heller, "Reducing anomalous reflection from complex absorbing potentials: A semiclassical approach," *Phys. Rev. A.*, vol. 103, Art. no. L041301, 2021.

[20] T. J. Cui, M. Q. Qi, X. Wan, J. Zhao, and Q. Cheng, "Coding metamaterials, digital metamaterials and programmable metamaterials," *Light Sci. Appl.*, vol. 3, e218-e218, 2014.

[21] Y. Liu, Y. Hao, K. Li, and S. Gong, "Wideband and polarization-independent radar cross section reduction using holographic metasurface," *IEEE*

Antennas Wirel. Propag. Lett., vol. 15, pp. 1028-1031, 2015.

[22] N. Yu, P. Genevet, M. A. Kats, F. Aieta, J. Tetienne, F. Capasso, and Z. Gaburro, "Light propagation with phase discontinuities: Generalized laws of reflection and refraction," *Science*, vol. 334, pp. 333-337, 2011.

[23] Y. Li, J. Zhang, S. Qu, J. Wang, H. Chen, L. Zheng, Z. Xu, and A. Zhang, "Achieving wideband polarization-independent anomalous reflection for linearly polarized waves with dispersionless phase gradient metasurfaces," *J. Phys. D: Appl. Phys.,* vol. 47, Art. no. 425103, 2014.

[24] Y. Li, J. Zhang, S. Qu, J. Wang, H. Chen, Z. Xu, and A. Zhang, "Wideband radar cross section reduction using two-dimensional phase gradient metasurfaces," *Appl. Phys. Lett.*, vol. 104, Art. no. 221110, 2014.

[25] F. Yuan, G.-M. Wang, H.-X. Xu, T. Cai, X.-J Zou, and Z.-H. Pang, "Broadband RCS reduction based on spiral-coded metasurface," *IEEE Antennas Wirel. Propag. Lett*., vol. 16, pp. 3188-3191, 2017.

Qingting He received the B.S. degree in Electronic Science and Technology from the Chengdu College of University of Electronic Science and Technology of China, Chengdu, China, in 2016. She is currently working toward the Ph.D. degree in Electronic Science and Technology at the University of Electronic Science and Technology of China, Chengdu, China.

Her recent research interests have focused on the numerical modeling of novel metamaterials and their applications in wave modulation, RCS reduction and wave absorbers.

Jianliang Xie received the Ph.D. degree in Material Physics and Chemistry from the University of Electronic Science and Technology of China (UESTC), Chengdu, China, in 2008.

He has worked as a Full Professor with the National Engineering Research Center of Electromagnetic Radiation Control Materials, UESTC. His research interests include magnetic material and devices, functional macromolecules, high-quality adherence systems, and electromagnetic absorbing structures.

Qian Liu received the B.S. degree in Materials Science and Engineering from Leshan Normal University, Leshan, China, in 2018. She received Master of Engineering in Electronic Science and Technology from the University of Electronic Science and Technology of China (UESTC), Chengdu, China, in 2021. She is currently working toward the Ph.D. degree in Microelectronics and Solid States Electronics at the University of Electronic Science and Technology of China (UESTC), Chengdu, China.

Her recent research interests include the structural design of novel metamaterials and their applications in electromagnetic wave modulation, orbital angular momentum, RCS reduction and wave absorbers.

Xin Yao received the B.S. degree in Electronic Science and Technology from Chongqing University of Posts and Telecommunications (CQUPT), Chongqing, China, in 2020. He is currently working toward the Ph.D. degree in Electronic Science and Technology at the University of Electronic Science and Technology of China (UESTC), Chengdu, China.

His recent research interests include the structural design of novel metamaterials and their applications in RCS reduction, de-coupling and sidelobe suppression for antenna arrays.

Zhi Wang is currently working toward the B.S. degree in Electronics and Electric Engineering with Information Engineering from University of Electronic Science and Technology of China (UESTC), Chengdu, China.

His recent research interests include RCS reduction and wave absorbers based on digital image processing, machine learning and smart heating in smart homes.

Haiyan Chen received the PH.D. degree in Microelectronics and Solid States Electronics from the University of Electronic Science and Technology of China (UESTC), Chengdu, China, in 2011. In 2015, he received the CSC (Chinese Scholarship Council) scholarship, and pursued study at the department of Engineering, University of Kentucky, Lexington, KY, USA, as a Visiting Scholarship.

Since 2012, he has been with the National Engineering Research Center of Electromagnetic Radiation Control Materials, UESTC, where he is now an Associate Professor. His research interests include artificial electromagnetic material and electromagnetic radiation control materials, particularly the study of electromagnetic discontinuous repair materials.

Fengxia Li received the B.S. degree in Electronic Information Science and Technology from Henan Polytechnic University, Jiaozuo, China, in 2015, and the Ph.D. degree in Microelectronics and Solid States Electronics from the National Engineering Research Center of Electromagnetic Radiation Control Materials, UESTC, in 2021.

Since 2021, she has been working with the School of Physics and Optoelectronic Engineering, Xidian University, as a Lecturer.

Her recent research interests include the structural design of novel metamaterials and their applications in electromagnetic wave modulation, frequency selective surfaces, RCS reduction, and wave absorbers.

Longjiang Deng received the M.S. degree in Electronic Material and Device from the University of Electronic Science and Technology of China (UESTC), Chengdu, China, in 1987.

Since then he has been working with UESTC, as a Lecturer, Associate Professor, and a Full Professor. He has authored/coauthored about 200 papers in peer-reviewed international journals and industry publications, and given many invited talks in international conferences. His research interests include electromagnetic wave absorbing material, infrared low emissivity and selective emissivity thin film, and microwave magnetic material.

Prof. Deng is a member of the Branch of Chinese Institute of Electronics on Microwave Magnetism, the Vice Director of the Special Committee of Chinese Institute of Electromagnetic Material, and a Member of the Editor Committee of *Chinese Journal of Functional Material*.